VII International Conference on Computational Methods for Coupled Problems in Science and Engineering
COUPLED PROBLEMS 2017
M. Papadrakakis, E. Oñate and B. Schrefler (Eds)

SOLVING AN INVERSE COUPLED CONJUGATE HEAT TRANSFER PROBLEM BY AN ADJOINT APPROACH

OLUWADAMILARE R. IMAM-LAWAL*, TOM VERSTRAETE* AND JENS-DOMINIK MÜLLER*

* School of Engineering and Materials Science.
Queen Mary, University of London. Mile End Road, E1 4NS, London, UK.
e-mail: o.r.imam-lawal@qmul.ac.uk, t.verstraete@qmul.ac.uk, j.mueller@qmul.ac.uk

Key words: Conjugate heat transfer, coupled, adjoint methods, inverse problems

Abstract. A framework for obtaining adjoint gradients for coupled conjugate heat transfer problems is presented. The framework is tailored to partitioned approaches in which separate solvers are used for the fluid and solid domains. The exchange of sensitivities between adjoint fluid and solid solvers is necessary in order to obtain gradients and how this is achieved is described. The effectiveness of the procedure is demonstrated by solving a conjugate heat transfer problem using a gradient based approach. The presented method can be extended to sensitivity analysis of multidisciplinary problems where both solvers offer adjoint derivatives.

1 INTRODUCTION

Conjugate Heat Transfer (CHT) describes the process of transferring heat between a fluid and solid and is ubiquitous in engineering applications, e.g the design of modern turbine blades, water cooling of combustion engines, and the heating of vehicles in hypersonic flow [1, 2].

CHT problems may be solved using a monolithic approach in which both fluid and solid equations are solved simultaneously by a single solver. Typically however the segregated or partitioned approach is adopted where separate solvers for the fluid and structure are loosely coupled through boundary conditions. These conditions need to be updated iteratively until the temperature and heat flux are continuous between the two domains [3]. One advantage of the partitioned approach is the flexibility of using different existing solvers for both domains [2, 3].

In this paper, we investigate an inverse heat transfer problem over a flat plate, in which the temperature on the bottom of the flat plate needs to be inferred from the temperature obtained at the interface between the flat plate and the fluid. Several examples of inverse CHT problems exist, however these problems are usually simplified into either inverse conduction [4, 5] or convection problems [6, 7, 8]. Ahamad and Balaji [9] consider both conduction and convection in their partitioned inverse problem. However, the problem is solved using artificial neural networks. To the authors knowledge, there exist very few inverse problems considering both conduction and convection which are solved with both a partitioned and gradient based approach.

The inverse problem is solved by formulating an optimization problem, which allows the use of classical direct methods to solve the physics involved. Here we use a partitioned method to predict the interface wall temperature starting from a guessed bottom temperature, while a gradient based method is used to reduce the deviation of this interface wall temperature with the desired one. The gradients of the objective w.r.t the control, i.e. the temperature specified on the bottom of the flat plate, are computed using an adjoint approach. Methods for the computation of multidisciplinary gradients have been proposed in [10, 11] and these methods are applied to two loosely coupled solvers leading to a fixed-point formulation of the adjoint system.

This paper is organised as follows: Section 2 first describes the direct problem, relevant equations, and the coupling procedure. The results of the direct problem are then presented and compared to an analytic solution to demonstrate the accuracy of the coupling procedure. Section 3 then describes the inverse problem, the derivation of adjoint gradients for the partitioned approach, and verification of the obtained gradients. The gradients are then used to solve the inverse problem using the steepest descent method. Conclusions are discussed in section 4.

2 DIRECT PROBLEM

The conjugate heat transfer problem to be considered in this work is the laminar flow over a flat plate with finite thickness. The free stream flow temperature is T_∞, while the bottom on the plate is maintained at a temperature T_b. Consequently, there is conjugate heat transfer at the interface between the solid plate and the fluid. The aim of the direct problem is to accurately compute the wall temperature T_w at the interface between the fluid and solid, which is unknown a priori and can only be computed by considering the coupled problem.

The fluid domain is governed by the Navier-Stokes equations for steady, laminar flow:

$$\frac{\partial U}{\partial t} + \frac{\partial F^j}{\partial x_j} \;=\; \frac{\partial G^j}{\partial x_j}. \tag{1}$$

where t denotes pseudo time and x_j, $j = 1, 2, 3$ are the cartesian coordinates. The sate vectors U, and the inviscid and viscous flux vectors F^j and G^j are defined as

$$U = \begin{bmatrix} \rho \\ \rho v_i \\ \rho e \end{bmatrix}, F^j = \begin{bmatrix} \rho v_j \\ \rho v_i v_j + p\delta_{ij} \\ (\rho e + p) v_j \end{bmatrix}, G^j = \begin{bmatrix} 0 \\ \tau_{ij} \\ v_j \tau_{ij} - q_j \end{bmatrix}. \tag{2}$$

where, ρ, p and v are the fluid density, pressure and velocity respectively, e the internal

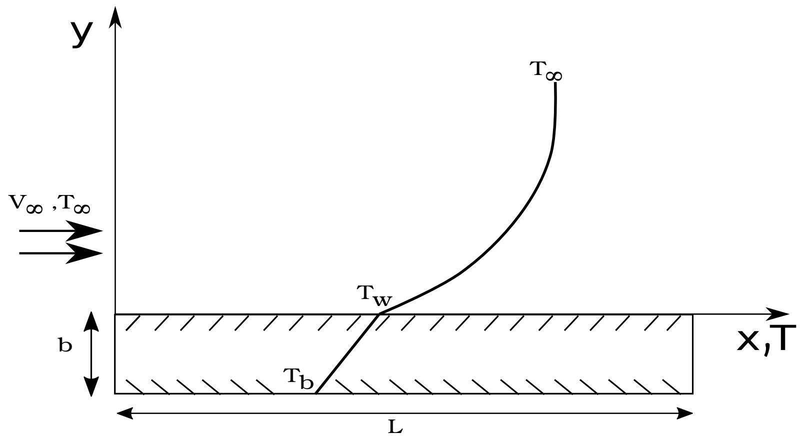

Figure 1: Description of the direct problem.

energy per unit mass, τ_{ij} the viscous stress, and q_j the heat flux. The solid domain is governed by Fourier's law

$$\lambda_s \nabla^2 T = 0, \tag{3}$$

where λ_s is the conductivity of the plate. The values of geometry, boundary conditions, and the Reynolds number of the case are shown in table 1.

Table 1: Table of parameters

Parameter	Value	units
b	0.01	m
L	0.2	m
M_∞	0.1	
P_∞	$1.03 \cdot 10^5$	Pa
T_∞	1000	K
λ_s	0.5555	W$m^{-1}K^{-1}$
Re_L	$1.132 \cdot 10^5$	

2.1 Coupling method

The problem is solved with a partitioned approach in which separate solvers are used for both domains and where boundary conditions are exchanged at each iteration to achieve continuity of temperature and heat flux across the domains. Different coupling methods exist depending on which boundary conditions are exchanged between both domains. In this work, we use the temperature forward flux back (TFFB) method [12], in which the wall heat flux distribution, q, is imposed as a boundary condition to the fluid domain, which after invoking the fluid solver $\mathbf{F}$ results in a wall, resulting in a wall temperature distribution, T (see equation 4). This temperature is subsequently imposed as boundary condition on the solid domain and the solid conduction solver, $\mathbf{S}$, then provides an updated heat flux distribution. This loop is continued until there is no change in the boundary conditions exchanged by both solvers.

$$\begin{aligned} T^i &= \mathbf{F}(q^i), \\ q^{i+1} &= \mathbf{S}(T^i). \end{aligned} \tag{4}$$

2.2 Simulation setup

The fluid domain is solved using the STAMPS flow solver, a vertex centered, finite volume solver, which solves the 3-D compressible RANS equation using unstructured grids. A second order accurate spatial discretisation is used with JT-KIRK implicit time stepping and automatic CFL ramping [13]. Two different fluid meshes are used to solve the direct problem in order to carry out a grid independence study. The coarser mesh is shown in Fig. 2 and details on the number of nodes in both meshes are shown in Table 2. The flat plate starts at position x=0 and ends at position x=0.2. The boundary conditions are also indicated in Fig. 2. A small inlet piece is added to the numerical domain in front of the flat plate to avoid inference of the boundary conditions on the results.

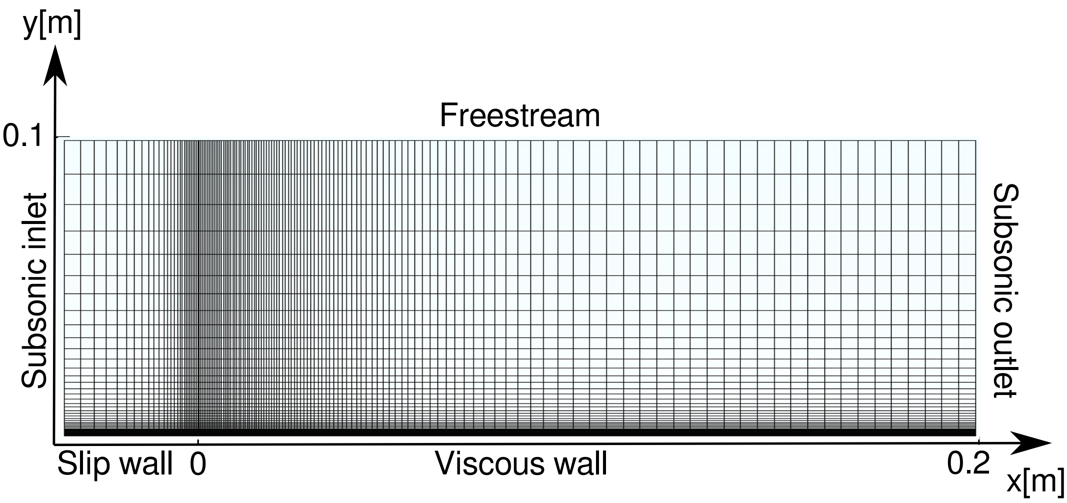

Figure 2: Mesh 1 and fluid simulation set up.

The solid domain is solved using a second order central spatial discretization and explicit time integration is achieved using a first order Euler scheme. A node-centred, structured grid with matching nodes at the interface between the fluid and solid domains is used to avoid interpolation during the exchange of boundary conditions, but in general the coupling procedure would allow for non-matching grids at the interface.

Table 2: Table showing the number of grid points in each part of the mesh

Mesh	Slip wall	Viscous wall	Fluid height
Mesh 1	24	113	97
Mesh 2	48	226	194

2.3 Direct problem results

The coupling procedure is first validated against the Luikov analytic solution for differential heat transfer to ensure the direct CHT problem is solved accurately. A comparison of the obtained streamwise wall temperature and the analytic temperature profile derived by Luikov [14] are shown in Fig. 3a. To check the convergence of the coupling procedure, we define as residual as

$$Res = \sqrt{\sum_{j=1}^{nNodes} (T^{i}_{jNode} - T^{i-1}_{jNode})^2}, \tag{5}$$

where i denotes the coupling iteration. The plot of the residual is shown in Fig. 3b.

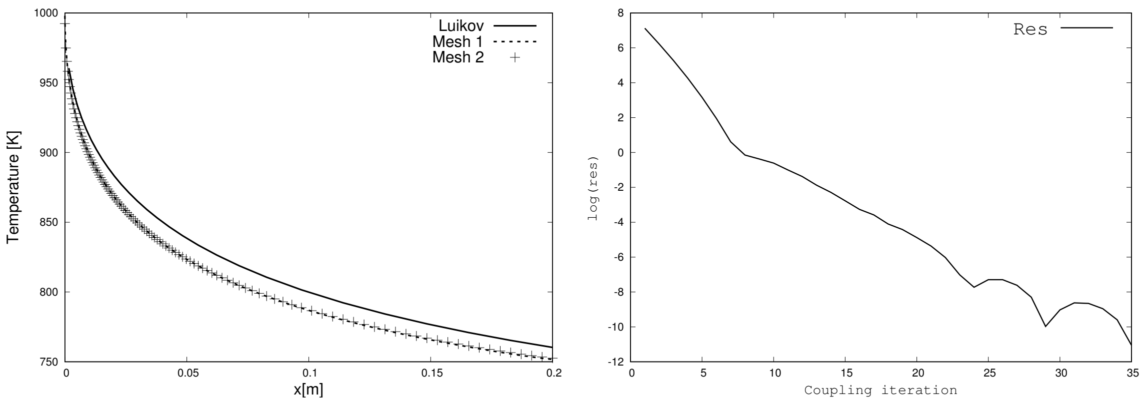

(a) Obtained T_w with $T_b = 600$ K. (b) Convergence of coupling iterations.

Figure 3: Temperature distribution and residual convergence plots of the direct solution.

The obtained temperature distribution shows good agreement with the analytic profile. The discrepancy between the obtained and the analytic temperatures may be because the Luikov solution is only an approximate solution where lateral heat transfer in the solid is not modeled. The results for both meshes also show grid convergence, therefore, in order to reduce the computational cost, Mesh 1 is used to solve the inverse problem.

3 INVERSE PROBLEM

In the inverse problem we seek the bottom temperature T_b which results in the best match for a given the interface wall temperature T_w. We define an objective function (J) as the difference between the given interface temperature (T_{target}) and the obtained interface temperature (T_x) for an estimated bottom temperature ($\tilde{T}_b$).

$$J = \frac{1}{2}\int_0^L (T_{target} - T_x)^2 dx. \tag{6}$$

The objective function depends implicitly on the bottom temperature T_b through the solution of the coupled problem. Each node at the bottom of the plate has an independent value of T_b specified as boundary condition, and is used in this work as a control variable (α) that needs to be changed to drive J to zero. As a result, the control variable α in the discrete problem is an array of size N, being 113 in the present work with Mesh 1.

The objective is hence to minimise equation (6) subject to the constraints of satisfying both the state equations of both domains (equations 1 - 3) and the convergence of the partitioned coupling scheme Eqn. (4) which we can rewrite at steady state in residual form:

$$\begin{aligned} R_f = & \quad T_w^\infty - \mathbf{F}(q_w^\infty) & = 0, \\ R_s = & \quad \mathbf{S}(T_w^\infty) - q_w^\infty & = 0, \end{aligned} \tag{7}$$

where the superscript ∞ denotes the final coupling iteration.

3.1 Minimisation problem

The inverse problem can be solved using a gradient based approach by driving the gradient of the objective w.r.t control variables to zero. Finite differences may be used to obtain the required gradients, however, the accuracy of the method is dependent on the step size, where a too large step size results in truncation errors due to the non-negligible higher order terms, and a too small step size results in numerical imprecision due to round off errors. Furthermore, the coupling algorithm would need to be run as many times we have control variables to obtain the sensitivity with respect to each control parameter.

Alternatively, both the fluid and solid solvers as well as the coupling procedure can be differentiated to obtain the gradients. The gradient of the objective function (sensitivity) w.r.t the control variables, α, is given as

$$\begin{aligned} \frac{dJ}{d\alpha} &= \int_0^L (T_{target} - T_w)\frac{dT_x}{d\alpha}dx, \\ &= -\sum_{j=1}^{N}(T_{target} - T_w)\frac{dT_x}{d\alpha}, \\ &= g^T u, \end{aligned} \tag{8}$$

where

$$\begin{aligned} g_i = & \quad T_{target_i} - T_{x_i} \quad \text{(column vector)}, \\ u_i = & \quad \frac{dT_{x,i}}{d\alpha} \quad \text{(column vector)}. \end{aligned}$$

Equation (9) requires a solve for u for every control variable. A perturbation of the bottom temperature (α) perturbs the heat flux distribution, which in turns perturbs the temperature distribution. This perturbation cascades through the entire coupling procedure and leads to a perturbation in the solution to the coupled problem. Nevertheless, upon convergence of the coupling method, equation (7) must be satisfied. Similarly, the total derivative of the system w.r.t to any control variable must be zero. This leads to the system of equations

$$\begin{aligned} \frac{\partial R_f}{\partial T_w^\infty}\frac{dT_w^\infty}{d\alpha} + \frac{\partial R_f}{\partial q_w^\infty}\frac{dq_w^\infty}{d\alpha} + \frac{dR_f}{d\alpha} &= 0 \\ \frac{\partial R_s}{\partial T_w^\infty}\frac{dT_w^\infty}{d\alpha} + \frac{\partial R_s}{\partial q_w^\infty}\frac{\partial q_w^\infty}{\partial \alpha} + \frac{dR_s}{d\alpha} &= 0, \\ \begin{bmatrix} \frac{\partial R_f}{\partial T_w^\infty} & \frac{\partial R_f}{\partial q_w^\infty} \\ \frac{\partial R_s}{\partial T_w^\infty} & \frac{\partial R_s}{\partial q_w^\infty} \end{bmatrix} \begin{bmatrix} \frac{dT_w^\infty}{d\alpha} \\ \frac{dq_w^\infty}{d\alpha} \end{bmatrix} &= \begin{bmatrix} -\frac{\partial R_f}{\partial \alpha} \\ -\frac{\partial R_s}{\partial \alpha} \end{bmatrix}. \end{aligned} \tag{9}$$

This can be rewritten as

$$\begin{aligned} \mathbf{A}u &= f, \\ u &= \mathbf{A}^{-1}f, \end{aligned} \tag{10}$$

where $\mathbf{A}$ is the extended Jacobian of the system. Solving this linear system once allows to compute the sensitivity by substituting for u in equation (9), which gives

$$\frac{dJ}{d\alpha} = g^T\mathbf{A}^{-1}f. \tag{11}$$

However, since the problem has multiple control variables α, this exercise needs to be repeated for each α, hence requiring N linear system solves (in this work 113). Additionally, the Jacobian matrix in equation (9) is not explicitly computed in the TFFB coupling approach used in the present work.

3.2 Adjoint equations

Regrouping the terms in equation (11) allows to introduce a new variable v as follows:

$$
\begin{aligned}
\frac{dJ}{d\alpha} &= (g^T\mathbf{A}^{-1})f, \\
&= v^T f, && (12) \\
&= \begin{bmatrix}\bar{T}_w & \bar{q}_w\end{bmatrix}\begin{bmatrix}-\dfrac{\partial R_f}{\partial \alpha} \\ -\dfrac{\partial R_s}{\partial \alpha}\end{bmatrix}, && (13)
\end{aligned}
$$

where v represents the adjoint values of temperature and heat flux $(\bar{T}_w, \bar{q}_w)$ and is the solutions of the linear system

$$
\begin{aligned}
\begin{bmatrix}\dfrac{\partial R_f}{\partial T_w}^T & \dfrac{\partial R_s}{\partial T_w}^T \\ \dfrac{\partial R_f}{\partial q_w}^T & \dfrac{\partial R_s}{\partial q_w}^T\end{bmatrix}\begin{bmatrix}\bar{T}_w \\ \bar{q}_w\end{bmatrix} &= \begin{bmatrix}\dfrac{\partial J}{\partial T_w} \\ \dfrac{\partial J}{\partial q_w}\end{bmatrix}, && (14) \\
\mathbf{A}^T v &= g, \\
v^T &= g^T\mathbf{A}^{-1}.
\end{aligned}
$$

The advantage of computing the sensitivity through equation (12) is that only one solve of the adjoint system (equation (14)) is required to obtain the adjoint variables regardless of the number of control variables.

The adjoint approach can also be obtained using reverse mode automatic differentiation and is the technique which is employed here. It results in an equivalent approach in which the Jacobian is not computed explicitly, rather the full forward run is repeated in reverse as illustrated in Fig. 4. The fluid state at each coupling iteration during the direct solve is stored and used to initialise the adjoint solve in the reverse coupling iteration. The accumulation of $\bar{\mathbf{T}}_\mathbf{b}$ yields the gradient values which are the solution to equation (12).

3.3 Gradient verification

To ensure the adjoint method is implemented correctly, a typical test is executed which compares the results with Finite Differences (FD). Although the accuracy of FD can be a significant issue, it can provide a reasonable indication of whether the adjoint code is implemented correctly. The obtained adjoint and FD gradients are compared in Fig. 5a.

The target temperature is obtained by solving the primal problem with a bottom temperature of 600K and is denoted as $T_{target}|_{T_b=600K}$. $\tilde{T}_b$ is taken as 400K and refers to the estimated bottom temperature that should yield T_{target} .

The adjoint and FD gradients show good agreement to plotting accuracy. Fig. 5b shows the convergence of the coupling procedure for the direct and adjoint solves. For the adjoint convergence, the same residual defined in equation (5) is used with the temperature values replaced by gradient values.

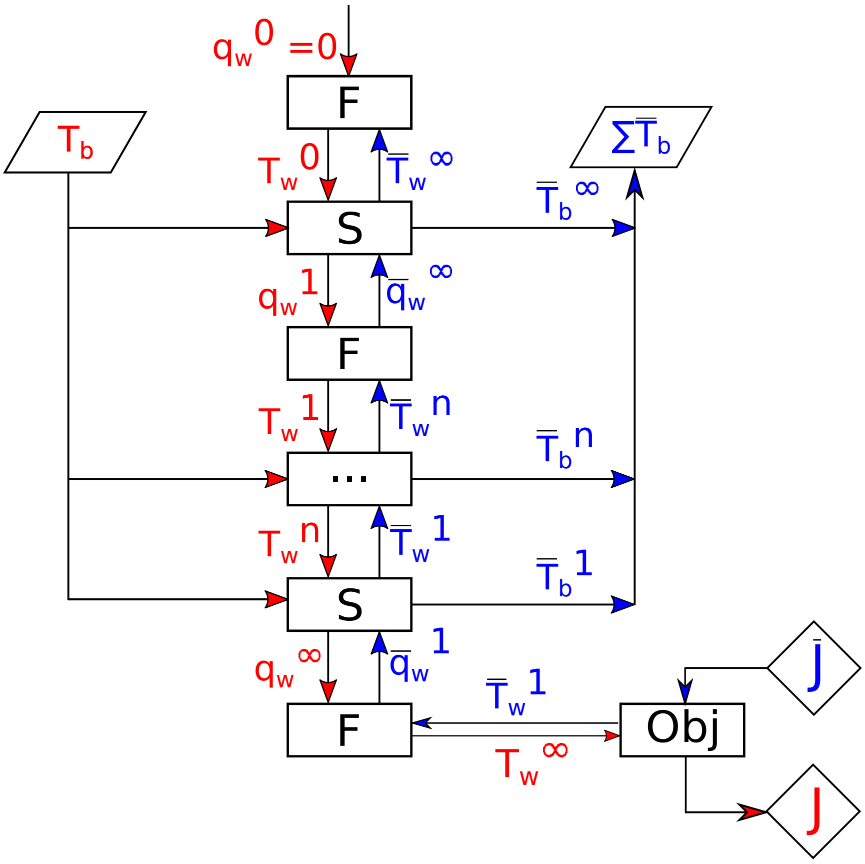

Figure 4: Coupling iterations (Direct = red, Adjoint = blue).

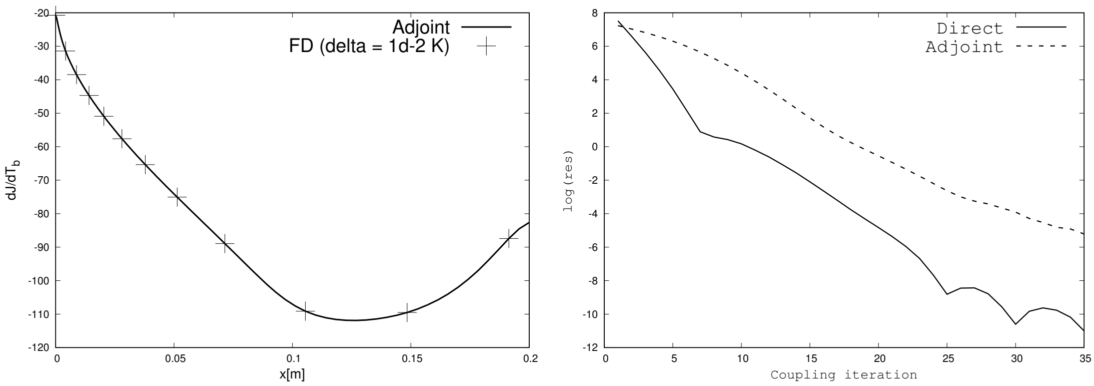

(a) Adjoint vs. FD gradients. (b) Convergence of coupling iterations.

Figure 5: Gradient comparison and coupling convergence for $\tilde{T}_b = 400\text{K}$ vs. $T_{target}|_{T_b=600K}$.

3.4 Results

The objective is minimised using the steepest descent algorithm which is run for 15 iterations. We define the difference between the temperatures obtained from the direct and inverse solution as

$$T_{\text{error}} = T_{\text{Target}} - T_{\text{Inverse}}, \tag{15}$$

The obtained wall temperature distributions and the error for each node are shown in figures 6a and 6b.

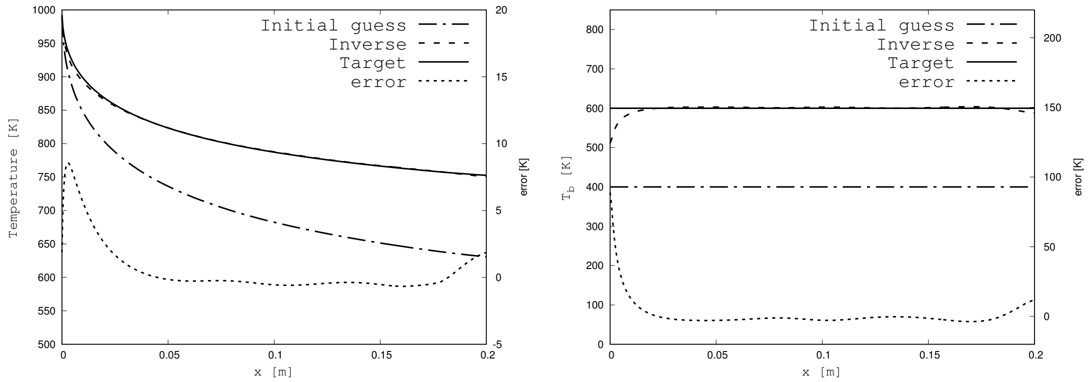

(a) T_w distribution. (b) T_b distribition.

Figure 6: Results of wall and bottom temperature distribution.

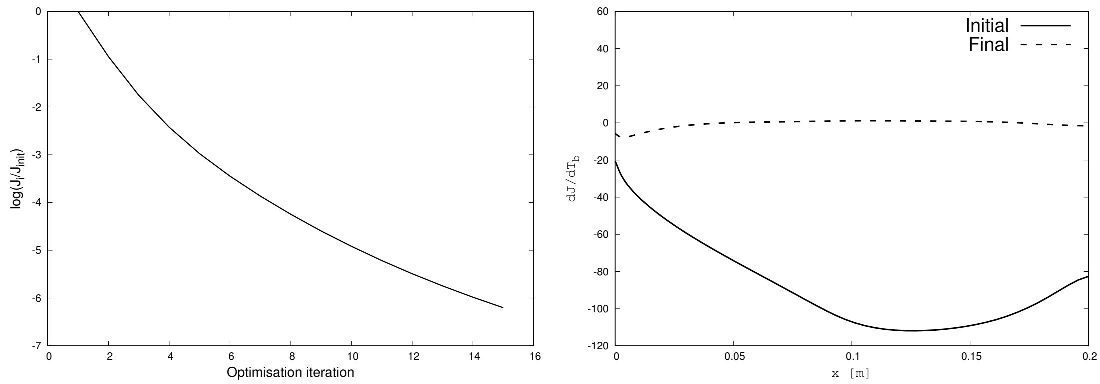

(a) Evolution of the objective function. (b) Gradients of objective w.r.t T_b.

Figure 7: Cost function and gradient plots for $\tilde{T_b} = 400\text{K}$ vs. $T_{target}|_{T_b=600K}$.

Fig. 6 shows that the inverse solution is significantly closer to the target than the initial values while Fig 7 shows that the values of the objective and sensitivities have been reduced considerably. The results show that the gradient computation procedure described Sec. 3.2 can be successfully utilised by optimisation algorithms. Consequently, the described procedure can be used to obtain sensitivities using any two adjoint solvers which provide the required multidisciplinary gradients.

4 CONCLUSION

This paper discusses the use of a partitioned approach to solve an inverse conjugate heat transfer problem. The partitioned method used is described in section 2 and validated with and analytic solution. In section 3, adjoint methods have been used to solve an inverse problem using a gradient based approach. The derivation of adjoint equations for the partitioned system was presented and the exchange of sensitivity information between the adjoint solvers in order to obtain multidisciplinary gradients was described. The description shows a framework capable of combining any two adjoint solvers in order to compute multidisciplinary gradients. The developed framework was successfully used in an optimisation algorithm to demonstrate its effectiveness. Future work will include the replacement of the simplified heat conduction solver with the reverse-differentiated open-source solver, Calculix. Additionally, the presented framework could be extended to shape optimisation problems involving CHT and multidisciplinary design optimisation.

REFERENCES

[1] Alok Majumdar and S.S. Ravindran. Numerical prediction of conjugate heat transfer in fluid network. *American Institute of Aeronautics and Astronautics*, 2010.

[2] V. Ganine, N.J. Hills, and B.L. Lapworth. Nonlinear acceleration of coupled fluid-structure transient thermal problems by anderson mixing. *International Journal for Numerical Methods in Fluids*, 71:939–959, 2013.

[3] Tom Verstraete and Sebastian Scholl. Stability analysis of partitioned methods for predicting conjugate heat transfer. *International Journal of Heat and Mass Transfer*, 101:852–869, 2016.

[4] Jianhua Zhou, Yuwen Zhang, J.K. Chen, and Z.C. Feng. Inverse estimation of surface heat condition in a three-dimensional object using conjugate gradient method. *International Journal of Heat and Mass Transfer*, 53:2643–2654, 2010.

[5] An inverse heat conduction problem with heat flux measurements. Tahar loulou and elaine p. scott. *International Journal for Numerical Methods in Engineering*, 67:1587–1616, 2006.

[6] Wen-Lih Chen and Yu-Ching Yang. On the inverse heat convection problem of the flow over a cascade of rectangular blades. *International Journal of Heat and Mass Transfer*, 51:4184–4194, 2008.

[7] Chen-Hung Huang and Wei-Chung Chen. A three-dimensional inverse forced convection problem in estimating surface heat flux by conjugate gradient method. *International Journal of Heat and Mass Transfer*, 43:3171–3181, 2000.

[8] Fu-Yun Zhao, Di Liu, Li Tang, Yu-Ling Ding, and Gaung-Fa Tang. Direct and inverse mixed convections in an enclosure with ventilation ports. *International Journal of Heat and Mass Transfer*, 52:4400–4412, 2001.

[9] Shaik Imran Ahamad and C. Balaji. Inverse conjugate mixed convection in a vertical substrate with protruding heat sources: a combined experimental and numerical study. *Heat and Mass Transfer*, 52:1243–1254, 2015.

[10] Antonio Fazzolari, Nicolas R. Gauger, and Joël Brezillon. Efficient aerodynamic shape optimization in mdo context. *Journal of Computational and Applied Mathematics*, 203:548–560, 2005.

[11] Joaquim R. R. A. Martins and John T. Wang. Review and unification of methods for computing derivatives of multidisciplinary computational models. *American Institute of Aeronautics and Astronautics*, 51, 2013.

[12] E. Divo, E. Steinthorsson, F. Rodriguez, A. J. Kassab, and J.S. Kappat. Glenn-ht/bem conjugate heat transfer solver for large-scale turbomachinery models. Technical Report NASA/CR-2003-212195, NASA, 2003.

[13] Shenren Xu, David Radford, Marcus Meyer, and Jens-Dominik Müller. Stabilisation of discrete steady adjoint solvers. *Journal of Computational Physics*, 2015.

[14] A. V. Luikov. Conjugate convective heat transfer problems. *International Journal of Heat and Mass Transfer*, 17:257–265, 1974.